PNAS

Supporting Information for

SRF transcriptionally regulates the oligodendrocyte cytoskeleton during CNS myelination

Authors: Tal Iram[1,2,7]*, Miguel A. Garcia[3]*, Jérémy Amand[5,6], Achint Kaur[1,2], Micaiah Atkins[1,2], Manasi Iyer[3], Mable Lam[3], Nicholas Ambiel[3], Danielle M. Jorgens[4], Andreas Keller[5,6], Tony Wyss-Coray[1,2], Fabian Kern[5,6,#], J. Bradley Zuchero[3,7,8,#]

Lead author:
J. Bradley Zuchero
email: zuchero@stanford.edu

This PDF file includes:

Figures S1 to S5
Legends for Dataset 1 to 3
Supplementary Materials and Methods
Supplemental References

Other supporting materials for this manuscript include the following:

Datasets 1 to 3

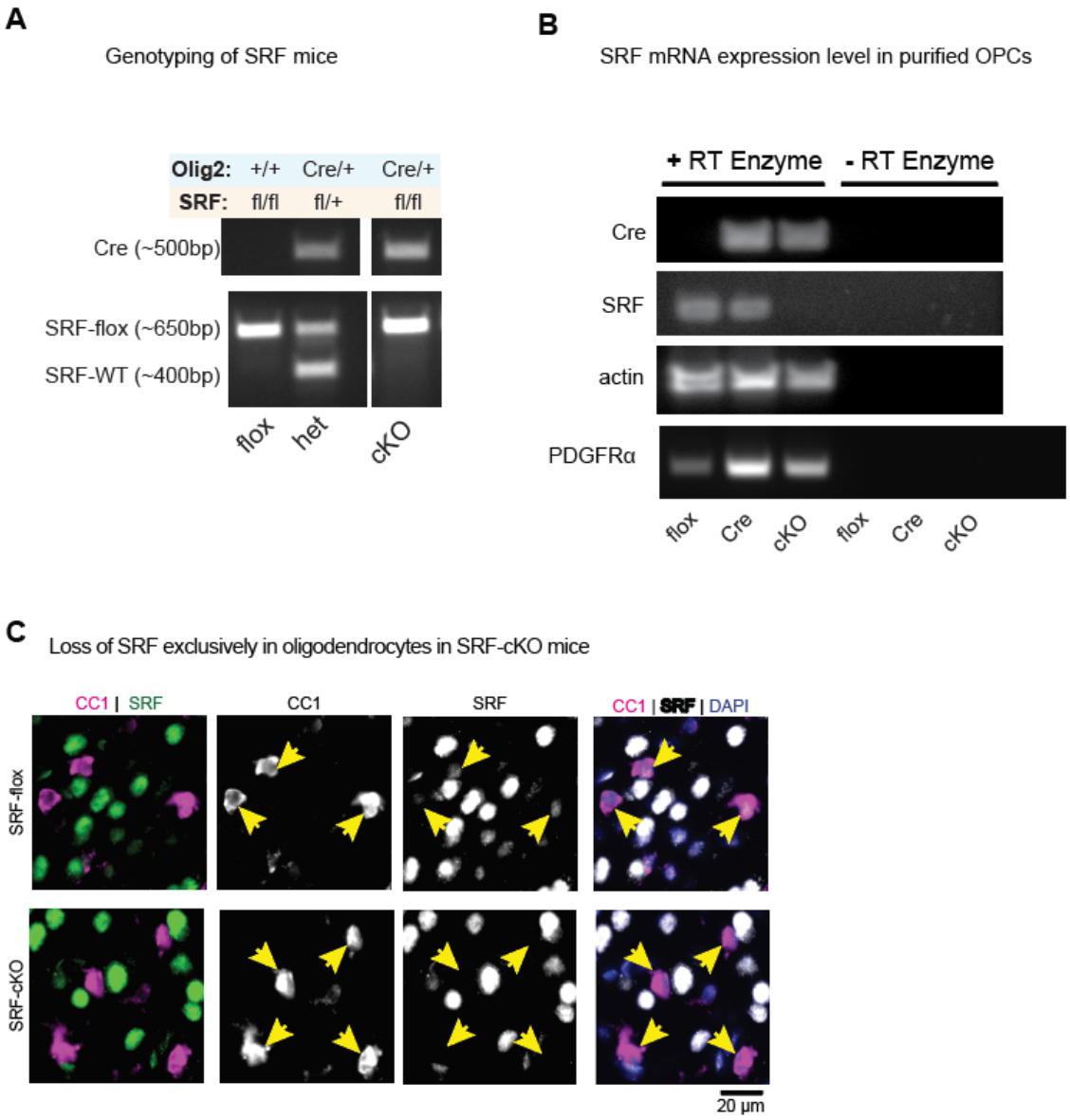

SI Appendix Fig.S1. Generation of SRF cKO mice.

A. Genotyping strategy and confirmation of Olig2-SRF-cKO mice.

B. Validation of loss of Srf from purified OPCs from Srf-flox, CRE mice and SRF-cKO mice by RT-PCR to detect expression of Cre, SRF, actin and Pdgfrα.

C. Validation of differential loss of Srf in mature oligodendrocytes ($CC1^+$ cells) in brain sections of SRF-flox and SRF-cKO mice by immunostaining.

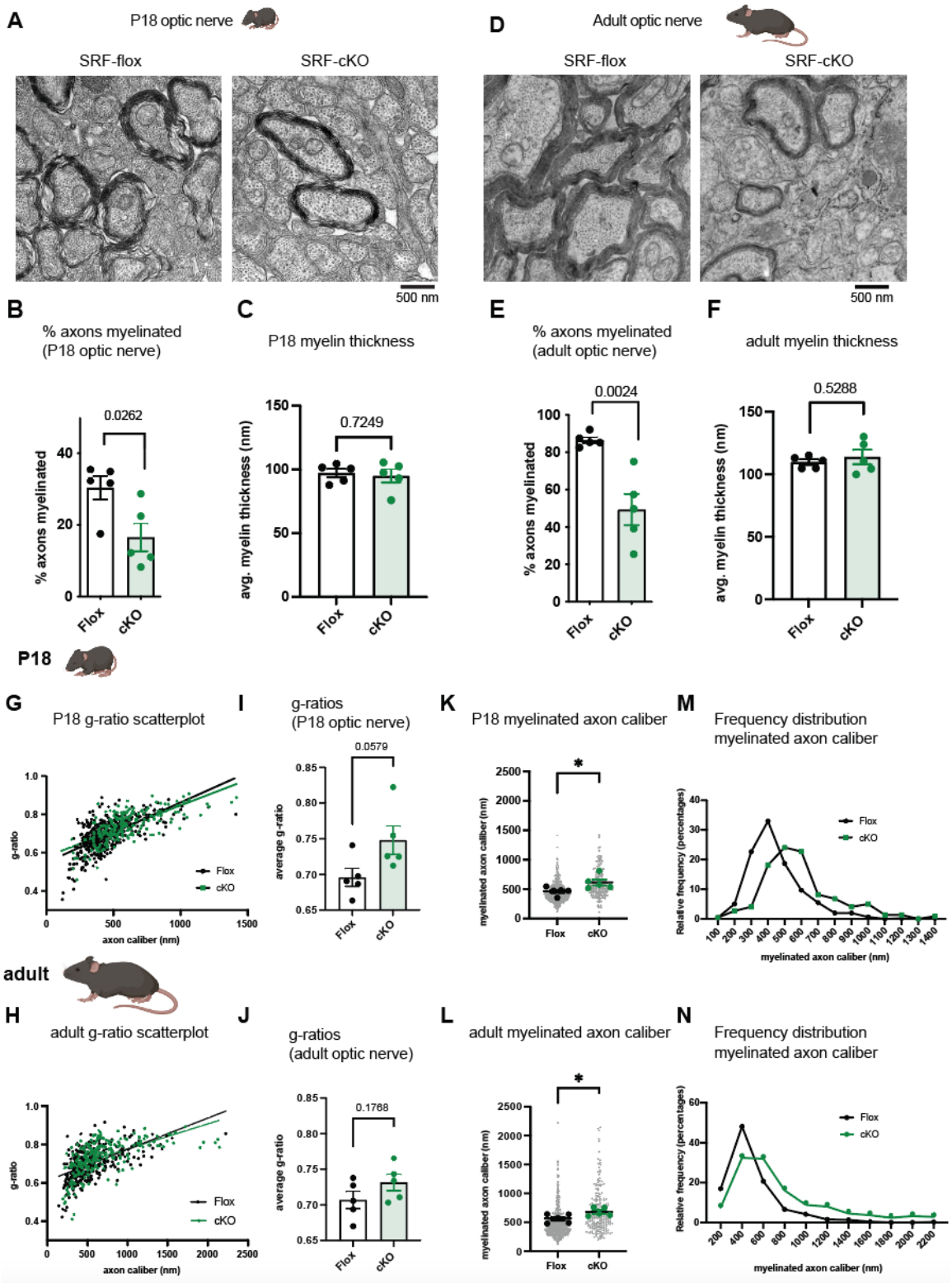

SI Appendix Fig.S2. EM analysis of optic nerves at P18 and adult SRF cKO mice.

A. Transmission electron microscopy of optic nerves from p18 SRF-flox and SRF-cKO. Scale bar represents 500nm.

B. Quantification of percent axons myelinated at P18. Each datapoint is an average of at least 700 axons per nerve from 5-6 micrographs spanning the entire nerve. n=5 animals from each genotype. Unpaired t-test.

C. Quantification of myelin thickness at P18. Each datapoint is an average of at least 700 axons per nerve from 5-6 micrographs spanning the entire nerve. n=5 animals from each genotype. Unpaired t-test.

D. Transmission electron microscopy of optic nerves from adult SRF- flox and SRF-cKO mice. Scale bar represents 500nm.

E. Quantification of percent axons myelinated in adult mice. Each datapoint is an average of at least 700 axons per nerve from 5-6 micrographs spanning the entire nerve. n=5 animals from each genotype. Unpaired t-test.

F. Quantification of myelin thickness in adult mice. Each datapoint is an average of at least 700 axons per nerve from 5-6 micrographs spanning the entire nerve. n=5 animals from each genotype. Unpaired t-test.

G-H. *g*-ratio of SRF-flox and SRF-cKO optic nerve myelinated axons as a function of axon caliber in P18 (G) and adult (H) mice.

I-J. Average *g*-ratios of SRF-flox and SRF-cKO optic nerve myelinated axons at P18 (I) and adult (J). n=5 mice per genotype at each timepoint.

K-L. Myelinated axon caliber of SRF-flox and SRF-cKO optic nerve at P18 (K) and adult (L). n=5 mice per genotype at each timepoint.

M-N. Frequency distribution of myelinated axon caliber of SRF-flox and SRF-cKO optic nerve axons at P18 (M) and adult (N).

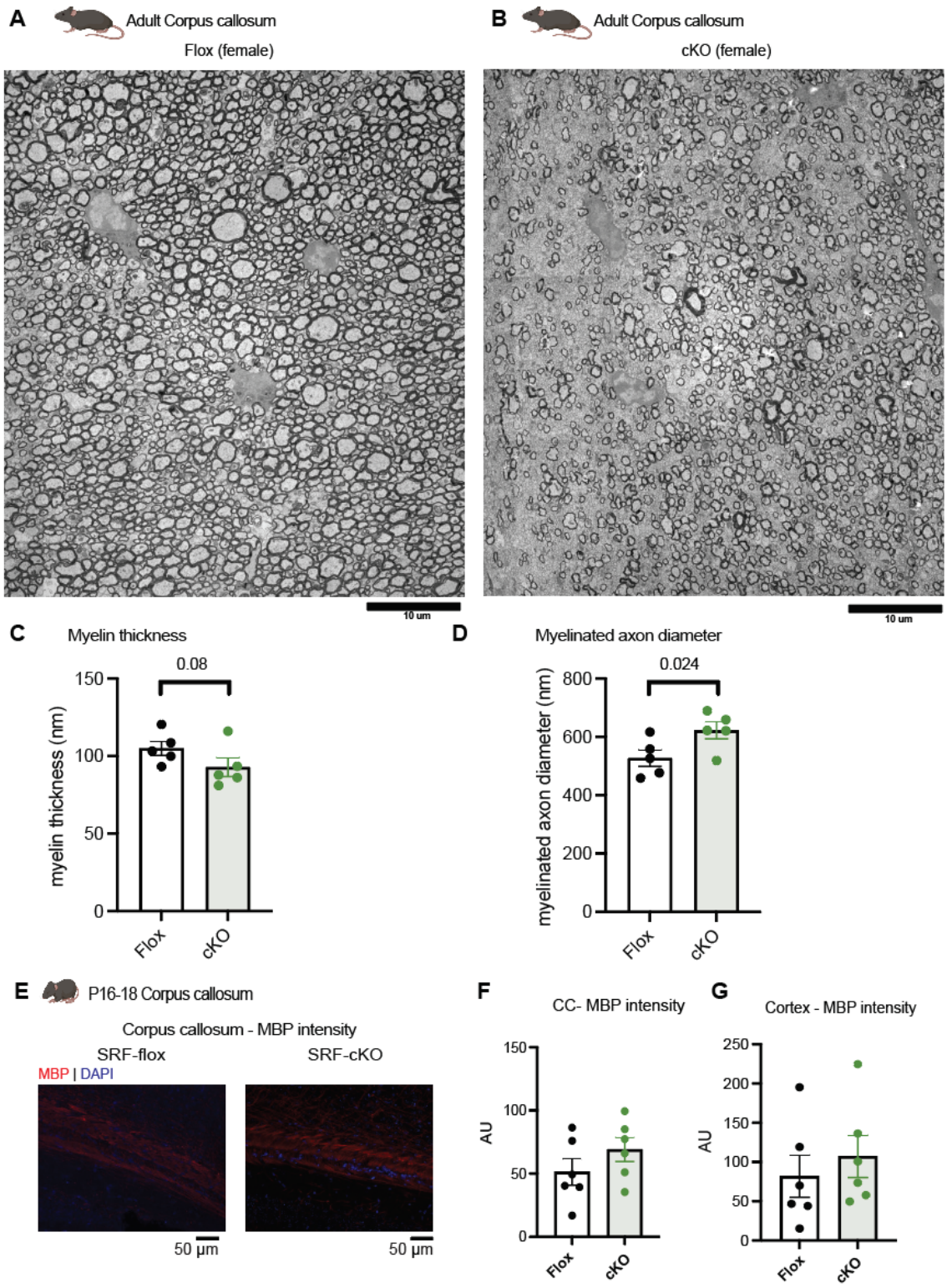

SI Appendix Fig.S3. Additional analysis of corpus callosum.

A. Representative transmission electron microscopy montage of corpus callosum of adult SRF-flox female mice. Scale bar represents 10μm.
B. Representative transmission electron microscopy montage of corpus callosum of adult SRF-cKO female mice. Scale bar represents 10μm.
C. Quantification of myelin thickness in adult corpus callosum. Each data point is an average of 100 myelinated axons measured per mouse. n=5 animals from each genotype. Unpaired t-test.
D. Quantification of the diameter of myelinated axons in adult corpus callosum. Each data point is an average of 100 myelinated axons measured per mouse. n=5 animals from each genotype. Unpaired t-test.
E. Representative images of MBP staining in corpus callosum of SRF-flox and SRF-cKO P16-P18 mice. Scale bar represents 50μm.
F. Analysis of the mean MBP intensity in the in the corpus callosum (CC) of SRF-flox and SRF-cKO mice. n=6 mice per genotype. Unpaired t-test.
G. Analysis of the mean MBP intensity in the cortex of SRF-flox and SRF-cKO mice. n=6 mice per genotype. Unpaired t-test.

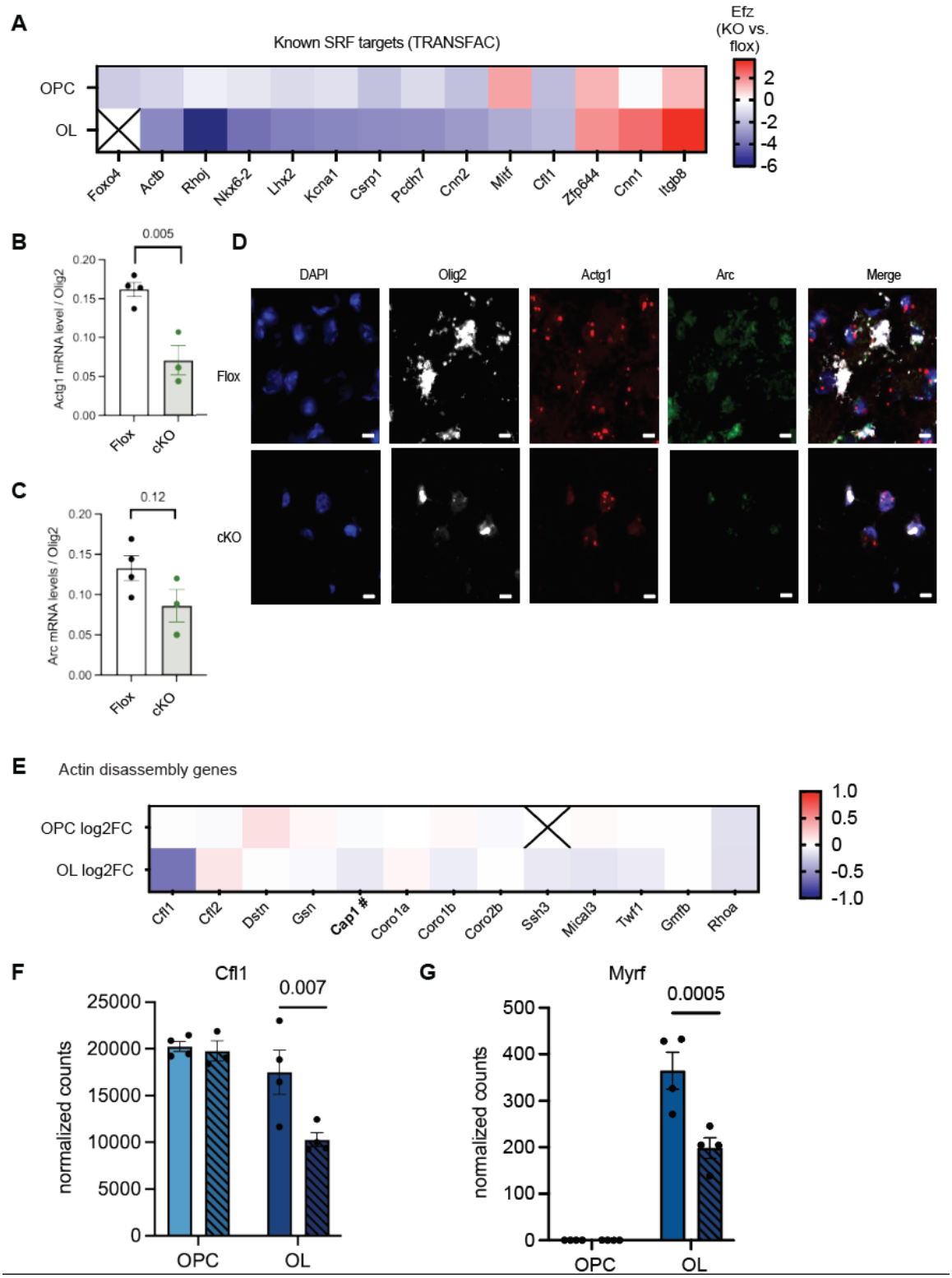

SI Appendix Fig.S4. SRF targets and actin disassembly genes in RNA-seq dataset.

A. Heatmap of selected SRF targets (predicted by the TRANSFAC database) showing the effect size of KO vs. flox OPCs and oligodendrocytes.

B. Quantification of Actg1 expression levels in Olig2^{+} nuclei in the cortex of P16/P18 SRF-Flox and SRF-cKO mice detected by RNAscope. n=4.

C. Quantification of Arc expression levels in Olig2^{+} nuclei in the cortex of P16/P18 SRF-Flox and SRF-cKO mice detected by RNAscope. n=4.

D. Representative images of DAPI, Olig2, Actg1, Arc and merge channel in SRF-Flox and SRF-cKO mice. Scale bar represents 10μm.

E. Heatmap of the main actin disassembly genes expressed by OPCs and oligodendrocytes [4,6] showing the log2FC of KO vs. flox OPCs and oligodendrocytes. # Indicates that Cap1 is a validated hit in the ChIP-seq experiment.

F. Normalized expression counts of Cfl1 in SRF- flox and SRF-KO OPCs and oligodendrocytes. OPC SRF-KO n=3. All the rest n=4. Statistics by DESeq2.

G. Normalized expression counts of Myrf in SRF- flox and SRF-KO OPCs and oligodendrocytes. OPC SRF-KO n=3. All the rest n=4. Statistics by DESeq2.

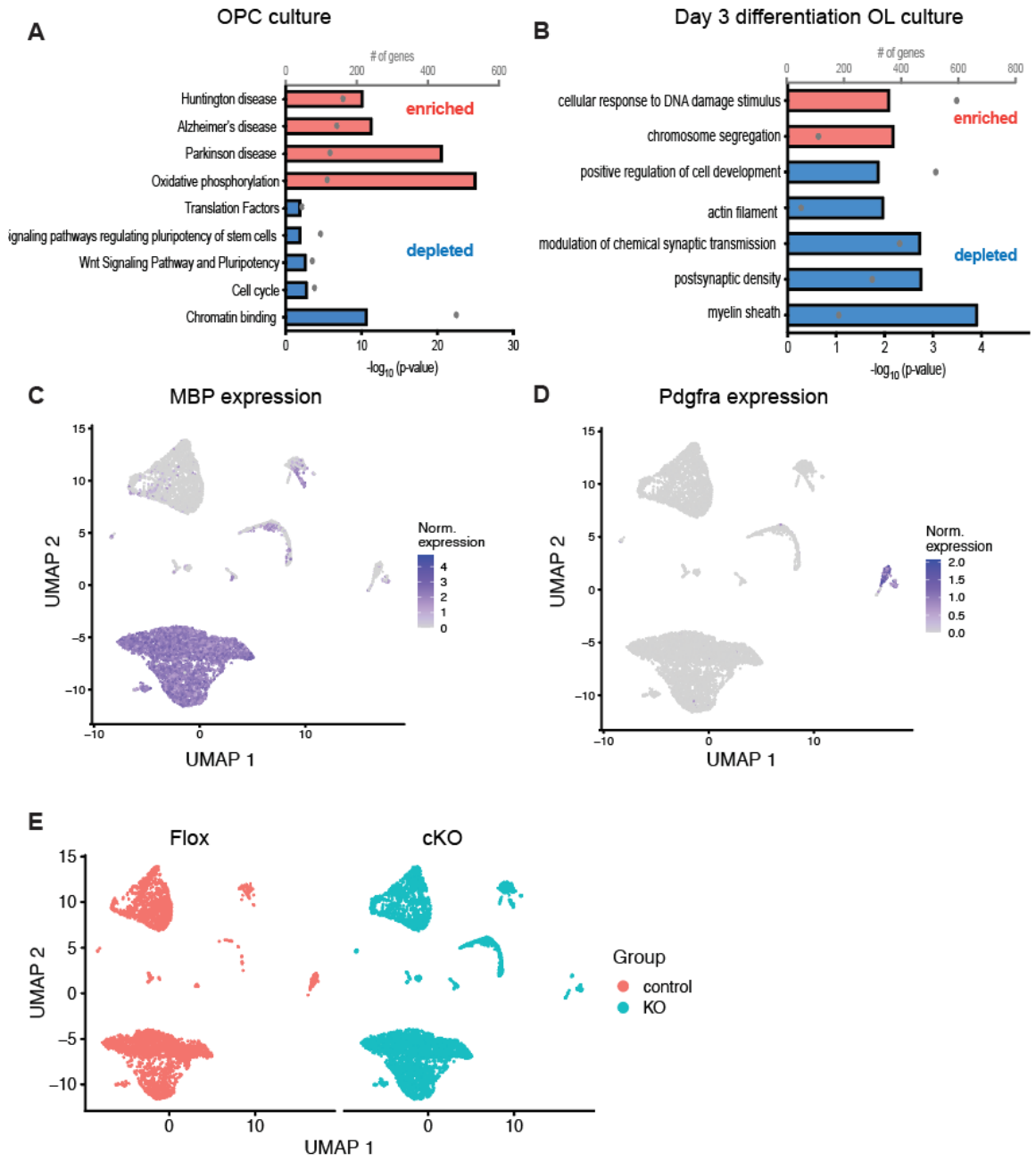

SI Appendix Fig.S5. Loss of SRF induces oligodendrocyte disease associated genes.

A. Pathways enriched (red) and depleted (blue) in SRF-KO OPCs bulk RNA-seq.

B. Pathways enriched (red) and depleted (blue) in SRF-KO oligodendrocytes bulk RNA-seq.

C. Scatter plot overlaying expression of the mature oligodendrocyte marker gene Mbp highly expressed in clusters 0 and 2.

D. Scatter plot overlaying expression of the OPC marker gene Pdgfrα highly expressed in cluster 5.

E. UMAP of clusters colored and split by group.

SI Appendix Dataset 1. SRF ChIP-seq peaks enriched in OPC or oligodendrocyte samples or both (common peaks) including motif analysis details.

SI Appendix Dataset 2. Normalized counts and summary statistics of bulk RNA-seq of SRF-cKO OPCs vs. SRF-flox OPCs.

SI Appendix Dataset 3. Normalized counts and summary statistics of bulk RNA-seq of SRF-cKO oligodendrocytes vs. SRF-flox oligodendrocytes.

Supplementary Material and Methods

RNA fluorescence in-situ hybridization (RNAscope)

C57Bl6/J (WT) mice were euthanized by decapitation with (P16) or without (P8) isoflurane anesthesia to allow for rapid collection of tissues for RNAscope. The brain was removed from the skull and immediately frozen on dry ice. Tissues were kept at –80 °C until sectioning. For tissue sectioning, frozen brains were mounted in O.C.T. compound (Thermo Fisher Scientific, 23-730-571) until sectioning. 10–12 µm thick sagittal sections were collected with a Leica CM3050 S cryostat preset to –20 °C. Sections were immediately transferred to cold Superfrost Plus (VWR, 48311-703) microscopy slide and stored at –80 °C until staining assays were performed.

RNAscope multiplex fluorescence (ACDbio) assays were completed according to the manufacturer's sample preparation manuals. Multiplex fluorescence kits (ACDbio, 320851) and the HybEZTM II Hybridization system (ACDbio, 321710) were used in all RNAscope assays. Fresh frozen tissue slices were fixed for 15 minutes in 4% paraformaldehyde solution (EMS, 15710) and serially dehydrated in ethanol washes immediately before assay.

After dehydration steps, samples were dried at room temperature for 20 minutes and then treated with pretreat IV (ACDbio, 320842) for 30 minutes. RNAscope probes were hybridized to target mRNAs, and the samples were treated with hybridization reagents Amp-FL 1-4 and counterstained with DAPI. Samples were covered with microscopy cover glass (Fisherbrand, 12-544-E) and mounted with Prolong Gold antifade mount (Invitrogen, 10144).

RNAscope Probe List:

Probe ID	**Species**	**ACDbio Cat#**
positive control (Polr2a, PPIB, UBC)	mouse	320881
negative control (Dapb)	Bacillus subtilis	320871
Pdgfra	mouse	480661
Olig2	mouse	447091
Srf	mouse	574761

Actb	mouse	316741
Actg1	mouse	400321
Arc	mouse	316911

For RNAscope imaging and analysis, slides were imaged with a Zeiss LSM 800 laser scanning confocal microscope using Zeiss Zen Blue software. A 63X oil objective was used to obtain Z-stack images of tissues. Specimens were blinded in the experiments and unblinded after imaging and analysis. Cells were chosen randomly for imaging based on DAPI or Olig2 expression without viewing the SRF channel. Quantification of the culture or in vivo RNAscope experiments was performed automatically using FishQuant (1). Except for cases in which a significant background signal was noted in a slide, the same threshold analysis settings were applied to all specimens within an experiment. Cell boundaries were determined using DAPI staining and mRNA localization.

Immunostaining of mouse tissue

Antibodies used in this study include rabbit-anti-SRF H-300 (Santa Cruz sc13029; 1:100), mouse-anti-CC1 (Millipore, OP980; 1:100), Rat-anti-MBP (Abcam, ab7349; 1:100; knockout-validated (2), rabbit-anti-NG2 (Millipore AB5320; 1:250), Rabbit-anti-Olig2 (Millipore AB9610, 1:500) and highly cross-absorbed Alexa Fluor 488-, 555-, 594-, or 647-labeled secondary antibodies (Thermo Fisher).

Tissues on slides were incubated with 10% goat serum (Thermo Scientific, PCN5000) in 0.1% Triton (Sigma, T8787) containing PBS for 1 hour. Primary antibody incubation was done in 1% goat serum in PBS overnight, then slides were rinsed 4 times for 30 minutes with 0.1% Triton containing PBS. Secondary antibody solution (Alexa Fluor 488, 1:500) was done at room temperature for 1-2 hours. Slides were rinsed four times with 0.1% Triton containing PBS for 30 minutes. Slides were counterstained with DAPI and mounted with Prolong Gold antifade mount (Invitrogen, 10144).

Transmission electron microscopy sample preparation

Optic nerve TEM

Transmission electron microscopy (TEM) was completed in the Stanford Cell Sciences Imaging Facility. Samples were prepared according to previously published protocols (3). Samples were initially washed in chilled Karlsson-Schultz fixative (2.5% glutaraldehyde, 4% PFA in phosphate buffer, pH 7.3) and incubated in 2% OsO4 for four hours at 4 °C. Samples were then serially dehydrated at 4 °C and embedded in EmBed812 (EMS, 14120). 80 nm sections were taken using an UC7 (Leica, Wetzlar, Germany) and were collected on formvar/Carbon coated 100 mesh Cu grids. Sections were then stained for 40 seconds in 3.5% uranyl acetate in 50% acetone followed by staining in Sato's lead citrate for 2 minutes. TEM images were obtained using a JEOL JEM-1400 120kV with a Gatan OneView 4k X 4k digital camera. Quantification of TEM images was performed manually using Fiji/Image-J, blinded to genotype.

Corpus callosum TEM

Perfusion and sectioning

Mice were deeply anesthetized then transcardially perfused by hand with 20 ml cold PBS, followed by 20 ml cold Karlsson-Schultz fixative (EM fixation buffer (3)) consisting of EM-grade 2.5% glutaraldehyde (EMS/Fisher, 50-262-08), 4% PFA (EMS/Fisher, 50-980-486), 13 mM NaH_2PO_4, 87 mM Na_2HPO_4, and 85.6 mM NaCl; total perfusion time was ~10 minutes per mouse. Brains were removed and post-fixed in cold (4° C) Karlsson-Schultz fixative until sectioning (at least 2 days post-fixing). Brains were sectioned sagittaly to 100-µm sections using a Leica VT1200S vibratome and sections were kept in cold Karlsson-Schultz fixative until further processing for EM.

High-pressure freezing with freeze substitution

Fixed brains were sectioned on a vibratome to 100 µm sagittal sections, and corpus callosum (immediately below cortex with some cortex included to aid in finding the same region in each sample) was punched out using a 1.5mm biopsy punch (AliMed Cat# 98PUN6-2) and subsequently stained using an osmium–thiocarbohydrazide–osmium (OTO) method (4, 5) in combination with microwave-assisted processing, followed by high-pressure freezing and freeze substitution (HPF–FS), as previously described (6). In brief, samples were stained with OTO, incubated with 2% aqueous uranyl acetate overnight and then subjected to HPF, followed by super-rapid FS (7) with 4% osmium tetroxide, 0.1% uranyl acetate and 5% ddH_2O in acetone; they were then thin-layer

embedded and polymerized in hard epon resin. Resin-embedded samples were precision cut off the glass slide and glued with cyanoacrylate onto a blank resin block for sectioning.

Transmission electron microscopy

Ultrathin sections of 90 nm were cut using a Leica UC6 ultramicrotome (Leica Microsystems) and collected onto formvar-coated 50-mesh copper grids or copper–rhodium slot grids. Because of native contrast from volume EM processing, no poststain was necessary. Sections were observed using a JEOL JEM-1400 120kV. Image montages were acquired using a Gatan OneView 4k X 4k digital camera capturing 8 x 8 montage images at 8000x magnification using SerialEM (University of Colorado Boulder), then reconstructed using the Etomo graphical user interface for IMOD 4.11 (University of Colorado Boulder; "Align Serial Sections / Blend Montages" feature). The resulting stitched tiff files were further analyzed for percent axons myelinated and *g*-ratios using Fiji/ImageJ. Percent axons myelinated were measured by hand using the Fiji Multi-point tool, and axon diameter/myelin thickness measurements were made with the line tool after setting the scale of the image to microns. All steps of EM processing, acquisition, and analysis were completed blinded to genotype. Due to regional heterogeneity of myelin content in the corpus callosum (especially in SRF-cKOs), we needed to score a large area (at least 1000 μm^2) to accurately assess percent axons myelinated; sample large fields of view are shown in SI Appendix, Fig.S3.

Purification and culture of oligodendrocytes

Primary oligodendrocyte precursor cells (OPCs) were purified by immunopanning from P5-P7 Sprague Dawley rat or P6-P7 transgenic mouse brains as previously described (8, 9). OPCs were typically seeded at a density of 150,000-250,000 cells/10-cm dish and allowed to recover and proliferate for 4 days in culture before lifting cells via trypsinization and distributing for proliferation or differentiation assays. All plasticware for culturing oligodendrocyte precursors were coated with 0.01 mg/ml poly-D-lysine hydrobromide (PDL, Sigma P6407) resuspended in water. All glass coverslips for culturing oligodendrocyte precursors were coated with 0.01 mg/ml PDL, which was first

resuspended at 100x in 150 mM boric acid pH 8.4 before diluting to 1x in water (PDL-borate). To proliferate primary oligodendrocyte precursors, cells were cultured in serum-free defined media (DMEM-SATO base medium) supplemented with 4.2 µg/ml forskolin (Sigma-Aldrich, Cat#F6886), 10 ng/ml PDGF (Peprotech, Cat#100-13A), 10 ng/ml CNTF (Peprotech, Cat#450-02), and 1 ng/ml neurotrophin-3 (NT-3; Peprotech, Cat#450-03) at 37°C with 10% CO2. To induce differentiation, cells were switched to DMEM-SATO base media containing 4.2 µg/ml forskolin (Sigma-Aldrich, Cat#F6886), 10 ng/ml CNTF (Peprotech, Cat#450-02), 40 ng/ml thyroid hormone (T3; Sigma-Aldrich, Cat#T6397) and (for mouse OPCs only) 1x NS21-MAX (R&D Systems AR008).

Confirming SRF knockout in OPCs/oligodendrocytes

We used the following primers to genotype SRF knockout mice: SRF-forward-2: TGCTGGTTTGGCATCAACT and SRF-reverse: GGCACTGTCTCAGGGTGTCT (WT SRF results in a 400 bp band; SRF-floxed allele results in a 650 bp band); Cre-forward: GCTAAGTGCCTTCTCTACACCTGC and Cre-reverse: GGAAAATGCTTCTGTCCGTTTG (presence of Cre indicated by the presence of a 500 bp band). For RT-PCR to analyze gene expression and test SRF knockout in OPCs, RNA was purified from immunopanned (95-99% pure) and proliferated OPC samples prepared as above, using the QIAGEN RNeasy Mini Kit. Note that SRF is expressed in cell types other than OPCs, so we used purified OPCs rather than total brain lysate for these experiments. Equal amounts of RNA (50-400 ng total) were reverse transcribed using SuperScriptIII (Invitrogen). Equal volumes from RT samples to be compared were then amplified using Platinum Taq (Invitrogen) with 26 PCR cycles, and sub-plateau reactions were analyzed by densitometry (NIH ImageJ). Primer sequences were SRF-RT-for: ACCAGTGTCTGCTAGTGTCAGC and SRF-RT-rev: CATGGGGACTAGGGTACATCAT.

Immunofluorescence of primary rat or mouse oligodendrocytes

Primary rat OPCs (WT) or primary mouse OPCs from SRF-flox and SRF-cKO littermate mice were harvested and proliferated for 1-4 days as described above in “Purification and Culturing of Cells”. Cells were seeded onto 12-mm glass coverslips (Carolina Biological

Supply No. 63-3029) coated with PDL-borate (see above) at a density of 10,000 cells/coverslip in differentiation media. At the specified day of differentiation, cell media was removed and coverslips were fixed with 4% formaldehyde in PBS for 15 minutes exactly, gently washed 3x in PBS, permeabilized with 0.1% Triton-X-100 in PBS for 3 minutes exactly, and gently washed 3x in PBS to remove Triton, all at room temperature (RT). Permeabilized cells were then blocked with 3% BSA (Sigma-Aldrich, A2153) in PBS for 20 minutes at RT. Antibody conditions for staining cultured oligodendrocytes were identical to those listed above in "Immunostaining of mouse tissue." Primary antibody incubation was performed at 4°C overnight in 3% BSA/PBS. Coverslips were incubated with secondary antibodies (1:1000 in 3% BSA/PBS) for 2 hours at RT. Actin filaments were stained using Alexa Fluor-conjugated phalloidin (Invitrogen; 50 nM in PBS) for 15 min exactly at RT. Cells were gently rinsed three times in PBS between each staining step. Finally, coverslips were mounted with Fluoromount G with DAPI (SouthernBioTech, 0100-20) on Superfrost microscopy slides (Fisherbrand, 12-550-143), air-dried overnight in the dark at RT, then stored at -20°C until shortly before imaging. Cells were imaged by widefield epifluorescence with a Zeiss Axio Imager M1 and Axiovision software using a 20x 0.8 NA Plan Apo objective (Carl Zeiss Microscopy). Images were acquired blinded to the genotype/experimental condition with identical illumination and acquisition conditions per biological replicate. Images were analyzed through batch processing in Fiji/Image J (10). Cells from 2-4 biological replicates were analyzed (2 coverslips per N served as technical replicates). To quantify actin filament content in cells, images were first color-thresholded to create cell-based ROIs. Then, mean cellular phalloidin intensity was measured, and background intensity of a region of the same image with no cells was subtracted from this intensity value.

ChIP-seq of OPCs and oligodendrocytes

Rat OPCs were allowed to proliferate for 6 days to reach 40 million cells in multiple 15cm plates. Half of the plates were fixed at the OPC stage while the rest were switched to differentiation medium and fixed on day 3 of differentiation. Replicates in this experiment were independent OPC preps. Chromatin immunoprecipitation was performed following iDeal ChIP-seq kit for Transcription Factors (Diagenode, Cat. No.

C01010055) using 7 cycles for chromatin shearing on a Bioruptor Pico sonicator (Diagenode, Cat. No. B01060001). Prior to sonication, each sample was split to 300ul reactions (containing each roughly 4 million cells) in 1.5 ml Bioruptor Microtubes (Cat. No. C30010016), sonicated, spun 16,000g for 10 min and 270ul of supernatant was collected to a new tube and stored in -80 deg. One aliquot of each sample was used for immunoprecipitation with 5ul of Rabbit-anti-SRF antibody that was validated for ChIP (SRF (D71A9) XP® Rabbit mAb, #5147) and an additional OPC and oligodendrocyte sample from each group for immunoprecipitation with an IgG control antibody (provided in the kit).

Libraries for next-generation sequencing were prepared using MicroPlex Library Preparation Kit v3 x48 rxns (C05010001, Diagenode) using 12 PCR cycles on a 96-plate thermal cycler (Biorad) and purified without size selection.

Library quantity and quality was assessed using a Bioanalyzer (Agilent) and Qubit. Libraries were pooled and sequenced on a Nextseq550 sequencer (Illumina) using single end 75bp for Read 1 and 8bp for index 1 and 8bp for Index 2 with a high output 75bp kit (20024906, Illumina).

In pilot studies, Chromatin Shearing Optimization kit - Low SDS (iDeal Kit for TFs) (Cat. No.C01020013) was used to determine optimal number of sonication shearing cycles to yield 200-300 bp fragments.

Bioinformatics analysis of ChIP-seq data

ChIP-seq data analysis was performed using the *nextflow-core ChIP-seq v1.2.1* pipeline (https://doi.org/10.5281/ZENODO.3966161) with default parameters, unless otherwise stated. In short, the pipeline first performs adapter trimming to the raw single-end reads using *Trim Galore* (option --nextseq=20) (https://www.bioinformatics.babraham.ac.uk/projects/trim_galore/). Next, reads were mapped to the *Rnor 6.0* rat genome obtained from Illumina iGenomes (Ensembl) using *BWA* (11). *MACS2* (12) was configured to call narrow peaks with a Benjamini-Hochberg FDR of 0.05 and an effective genome size of 2×10^9. *HOMER* (13) was then used to annotate peaks with information from the closest known genomic feature based on the Ensembl database. Consensus peaks for OPC and oligodendrocytes were aggregated by

considering peaks present in at least one replicate of the respective cell type. We performed known and *de novo* motif detection in the -250 to +250 nt regions around detected peaks using *MEME-ChIP (14)*. Next, FIMO (14) was used to get individual motif matches for MEME-ChIP results. The matrix of peak intensity around transcription start sites (TSS) was calculated using *deepTools* (15). Data transformation and plotting were performed using R v4.1.3.

RNA-seq of OPCs and oligodendrocytes

Mouse OPCs were purified from brains of SRF floxed by immunopanning as described above for rat OPCs. On day 3 of the culture, SRF-f/f OPCs were split and plated in 12-well plates at a density of 30K per well. When the cells were in suspension in proliferation media before plating, $1*10^{10}$ viral genomes of AAV DJ-CMV eGFP-deleted cre (GVVC-AAV-62) or AAV DJ-CMV eGFP-cre (GVVC-AAV-63) (both generated by the Stanford Gene Vector and Virus Core). The following day, media was fully replaced and 48hrs after infection media was removed and the plate was flash frozen on dry ice and kept in -80 deg. For CRE induction in oligodendrocytes, on day 5 after isolation, SRF-f/f OPCs were plated at a density of 35,000 cells per well in a 12-well plate. On day 6, cells were infected with 5.6-6.6 x 10^8 viral units of a lentivirus-CRE-IRES-GFP or GFP control. On day 7, media was replaced to differentiation media and on day 3 of differentiation the media was removed and plates were frozen at -80.

For RNA extraction, cells were scraped with RLT buffer and RNA was extracted with the RNeasy Plus Micro kit (Qiagen, 74034). cDNA and library synthesis were done inhouse using the Smart-seq2 protocol as previously described (16) (detailed protocol at https://doi-org.laneproxy.stanford.edu/10.17504/protocols.io.2uvgew6) with several modifications. Due to the low input RNA content, 2µl of RNA extracted from sorted nuclei was reversed transcribed using 18 cycles. Following bead cleanup using 0.7x ratio with AMPure beads (A63881, Fisher), cDNA concentration was measured using the Qubit 1x dsDNA HS kit (Q33231) and normalized to 0.4 ng/µl as input for library prep. 0.4 µl of each normalized sample was mixed with 1.2 µl of Tn5 Tagmentation mix (0.64 µl TAPS-PEG buffer (PEG 8000, V3011 , PROMEGA, and TAPS-NaOH pH8.5, BB-

2375, Boston Bioproducts), 0.46 µl H2O and 0.1 µl Tn5 enzyme (20034198, Illumina)), then incubated at 55 °C for 10 min. The reaction was stopped by adding 0.4 µl 0.1% sodium dodecyle sulfate (Fisher Scientific, BP166-500). Indexing PCR reactions were performed by adding 0.4 µl of 5 µM i5 indexing primer (IDT), 0.4 µl of 5 µM i7 indexing primer (IDT), and 1.2 µl of KAPA HiFi Non-Hot Start Master Mix (Kapa Biosystems) using 12 amplification cycles. Libraries were purified using two purification rounds with a ratio of 0.8x and 0.7x AMPure beads. Library quantity and quality was assessed using a Bioanalyzer (Agilent) and Qubit. All steps were done manually using 8-strip PCR tubes and PCR reactions were carried out on a 96-plate thermal cycler (Biorad). Libraries were pooled and sequenced on a Nextseq550 sequencer (Illumina) using single end 63bp for Read 1 and 12bp for index 1 with a high output 75bp kit (20024906, Illumina). Libraries were sequenced to a depth of at least >10 million reads per sample.

Bioinformatics analysis of RNA-seq data

Raw sequencing files were demultiplexed and known adapters were trimmed with bcl2fastq. Data analysis of raw sequencing data was performed using the nextflow-core RNA-seq pipeline v3.0. Briefly, the core workflow of the pipeline maps filtered reads against the species reference genome using STAR and computes transcript counts using RSEM. For nuclear RNA-seq data, a custom reference genome was created where exon sequences in GTF files were modified to include all introns per transcript and used for the mapping instead. For mouse and rat sequencing data the reference genome GRCm38 and Rnor 6.0 provided by Illumina igenomes were used, respectively. All gene annotations were based on the Ensembl database. Obtained raw gene transcript counts per sample were loaded into DESeq2, performing normalization for transcript length and sequencing depth, and differential expression analysis with standard settings. Effect sizes for each gene were computed based on normalized counts computed by DESeq2 using the function cohen.d of the R package effsize. Gene set enrichment analysis was performed using GeneTrail 3 using BH-FDR p-value adjustment with all remaining parameters kept at default.

Single-nucleus isolation, library prep and data analysis

Each 10x sample consisted of a pool of a pre-frontal cortex white matter biopsy punch of one 10 month old male and one female. Pre-frontal cortex was dissected using a 1.5mm biopsy punch (Alimed, 98PUN6-2) after serial sectioning at freezing temperatures as previously described. Punches were stored at -80°C until further processing. Nuclei were isolated with EZ Prep lysis buffer (Sigma, NUC-101) in a 2 ml glass dounce tissue grinder (Sigma, D8938) and homogenized by hand 25 times with pestle A followed by 25 times with pestle B, following the manufacturers instructions. After the final wash, the pellet was resuspended with 4 ml chilled PBS and filtered through a 35-um cell strainer into a 5 ml round bottom FACS tube (Corning, 352235) and centrifuged at 300 x g for 10 minutes at 4°C. Pellet was resuspended in 100 ul PBS containing 1% BSA (Thermo Fisher, BP9700100) with 1/250 647-anti-NeuN and was placed on a shaker on ice for 30 min. Following a wash, pellet was resuspended in PBS containing 1% BSA (Thermo Fisher, BP9700100), 0.2 ul Hoechst dye (Thermo Fisher, H3570), and 2 ul recombinant RNase inhibitor (Takara, 2313B) and 15,000 single $NeuN^-$ nuclei were sorted on a MA900 Sorter (Sony Biotechnology) into 1.5 ml DNA lo-bind tubes (Eppendorf, 022431021) containing 1 ml buffer mix with PBS, UltraPure BSA (Thermo Fisher, AM2618), and RNase inhibitor (Takara, 2313B).

Library preparation was prepared following the Chromium Single Cell 3' GEM & Gel Bead Kit v3.1 and Library Construction Kit v3 (10X Genomics) manufacturer's protocol. Nuclei and master mix solution was adjusted to target 10,000 nuclei per sample and loaded on a standard Chromium Controller (10X Genomics, 1000204) according to manufacturer protocols. We applied 12 PCR cycles to generate cDNA and 14 PCR cycles for library generation. Quality control of cDNA and libraries was conducted using a High Sensitivity D5000 ScreenTape (Agilent) at the Stanford Knight Initiative Facility. Illumina sequencing of the resulting libraries was performed on an Illumina NextSeq 550 (Illumina) using a High output Kit v2.5 (150 cycles, 20024907).

Computational processing of single-nucleus 10x libraries was performed as described previously using a slightly adapted workflow (17). First, we performed gene-wise ambient RNA removal using SoupX (18) (v1.6.2), applying the automatic contamination estimation

strategy on each of the raw count matrices obtained from CellRanger (v7.0.0) (10x Genomics). The gene-wise corrected count matrices were then filtered for low-quality and background cells using the default CellRanger algorithm. We then further excluded cells with 200 or fewer detected unique molecular identifiers (UMIs) and removed genes detected in fewer than 5 cells from further consideration. Resulting per-sample matrices were analyzed with DoubletFinder (19) (v2.0.3) to identify potentially contaminating populations of doublets and multiplets. Automatic estimation for the parameter pK was used with the first 20 principal components, setting pN and the expected doublet rate to 0.25 and 0.15, respectively. We then removed from each sample all cells expressing 5000 or more features, expressing 5% or more mitochondrial RNA, or being classified as 'Doublet' by DoubletFinder. After filtering, both samples contain a total of 9,093 high-quality nuclei. Subsequently, we normalized the cell count matrices for each sample using scTransform (20) (v.0.3.5) with default parameters. Following the official Seurat (v4.3.0) documentation to integrate samples using a scTransform-based workflow, we applied the functions *SelectIntegrationFeatures*, *PrepSCTIntegration*, *FindIntegrationAnchors*, and *IntegrateData* on 3000 features and 30 dimensions. Dimension reduction and clustering were then performed on the integrated assay using RunPCA, FindNeighbors, FindClusters, and RunUMAP in order with 20 significant dimensions, a clustering resolution of 0.3, and all other parameters set at default. Cell clusters were manually annotated using markers from previously published data sets. For down-stream cluster/cell type marker and differential gene expression analysis, we similarly followed our previous approach (17) using MAST (v1.24.0).

Supplemental References

1. F. Mueller *et al.*, FISH-quant: automatic counting of transcripts in 3D FISH images. *Nat Methods* **10**, 277-278 (2013).
2. J. B. Zuchero *et al.*, CNS myelin wrapping is driven by actin disassembly. *Dev Cell* **34**, 152-167 (2015).
3. W. Mobius, K. A. Nave, H. B. Werner, Electron microscopy of myelin: Structure preservation by high-pressure freezing. *Brain Res* **1641**, 92-100 (2016).
4. P. L. Friedman, M. H. Ellisman, Enhanced visualization of peripheral nerve and sensory receptors in the scanning electron microscope using cryofracture and osmium-thiocarbohydrazide-osmium impregnation. *J Neurocytol* **10**, 111-131 (1981).
5. M. C. Willingham, A. V. Rutherford, The use of osmium-thiocarbohydrazide-osmium (OTO) and ferrocyanide-reduced osmium methods to enhance membrane contrast and preservation in cultured cells. *J Histochem Cytochem* **32**, 455-460 (1984).
6. A. J. Ewald *et al.*, Mammary collective cell migration involves transient loss of epithelial features and individual cell migration within the epithelium. *J Cell Sci* **125**, 2638-2654 (2012).
7. K. L. McDonald, R. I. Webb, Freeze substitution in 3 hours or less. *J Microsc* **243**, 227-233 (2011).
8. B. Emery, J. C. Dugas, Purification of oligodendrocyte lineage cells from mouse cortices by immunopanning. *Cold Spring Harb Protoc* **2013**, 854-868 (2013).
9. J. C. Dugas, A. Ibrahim, B. A. Barres, The T3-induced gene KLF9 regulates oligodendrocyte differentiation and myelin regeneration. *Mol Cell Neurosci* **50**, 45-57 (2012).
10. J. Schindelin *et al.*, Fiji: an open-source platform for biological-image analysis. *Nat Methods* **9**, 676-682 (2012).
11. H. Li, R. Durbin, Fast and accurate short read alignment with Burrows-Wheeler transform. *Bioinformatics* **25**, 1754-1760 (2009).
12. Y. Zhang *et al.*, Model-based analysis of ChIP-Seq (MACS). *Genome Biol* **9**, R137 (2008).
13. S. Heinz *et al.*, Simple combinations of lineage-determining transcription factors prime cis-regulatory elements required for macrophage and B cell identities. *Mol Cell* **38**, 576-589 (2010).
14. T. L. Bailey, J. Johnson, C. E. Grant, W. S. Noble, The MEME Suite. *Nucleic Acids Res* **43**, W39-49 (2015).
15. F. Ramirez *et al.*, deepTools2: a next generation web server for deep-sequencing data analysis. *Nucleic Acids Res* **44**, W160-165 (2016).
16. T. Iram *et al.*, Young CSF restores oligodendrogenesis and memory in aged mice via Fgf17. *Nature* **605**, 509-515 (2022).
17. S. Herppich *et al.*, Zfp362 potentiates murine colonic inflammation by constraining Treg cell function rather than promoting Th17 cell differentiation. *Eur J Immunol* **53**, e2250270 (2023).
18. M. D. Young, S. Behjati, SoupX removes ambient RNA contamination from droplet-based single-cell RNA sequencing data. *Gigascience* **9** (2020).

19. C. S. McGinnis, L. M. Murrow, Z. J. Gartner, DoubletFinder: Doublet Detection in Single-Cell RNA Sequencing Data Using Artificial Nearest Neighbors. *Cell Syst* **8**, 329-337 e324 (2019).
20. C. Hafemeister, R. Satija, Normalization and variance stabilization of single-cell RNA-seq data using regularized negative binomial regression. *Genome Biol* **20**, 296 (2019).